Low-frequency magnetoacoustic resonance of transverse waves in the presence of an inhomogeneous internal field

L. K. Zarembo and S. N. Karpachev

M. V. Lomonosov State University, Moscow
(Submitted 3 February 1987)
Zh. Eksp. Teor. Fiz. **93**, 1499–1507 (October 1987)

Linear and nonlinear magnetooptic resonances are excited in small regions of a crystal magnetized to saturation in the presence of an inhomogeneous internal field. This makes it possible to reconstruct the structure of the internal field from the resonance profile. A low-frequency (tens of megahertz) magnetoacoustic resonance can be observed in crystals for which the intrinsic width of a ferromagnetic resonance line is sufficiently small. The resonant increase in the absorption coefficient α_r/α (at 30 MHz) is considerably less than the resonant increase in the nonlinear parameter Γ_r/Γ: in the case of a manganese zinc spinel it was found that $\alpha_r/\alpha \approx 2$ and $\Gamma_r/\Gamma \approx 400 \pm 100$; in the case of yttrium iron garnet it was found that $\alpha_r/\alpha \approx 50$ and that the nonlinear parameter has a giant value $\Gamma_r/\Gamma \approx 10^5$–$10^6$.

A direct magnetoacoustic resonance (MAR) in magnetic materials represents synchronous excitation of a spin wave under the action of an acoustic wave, manifested by a strong increase in the absorption of the latter wave;[1] it was first predicted in 1956 by Akhiezer, Turov, and Irkhin and then investigated experimentally by a number of authors.[2–7] These investigations were carried out in the frequency range 10^8–10^9 Hz mainly on yttrium iron garnet (YIG) crystals using longitudinal waves. The investigations were concerned with the conditions for the excitation of the MAR (nature of the waves, MAR anisotropy, relative orientations of the directions of propagation and the external field),[2–4,6] intrinsic MAR (in the absence of an external field) in anisotropy fields,[5] and nonlinear effects associated with the MAR.[7] In spite of the fact that some of the investigations were carried out on nonelliptic samples with inhomogeneous internal fields, these fields have not received sufficient attention. However, it should be pointed out that the problem of electromagnetic excitation of spin waves and their conversion into elastic waves in the presence of an inhomogeneous field was considered in Ref. 8.

It was shown in Ref. 7 that in the case of a nonlinear MAR the line representing the second longitudinal harmonic splits into a doublet with $\Delta H_d = f/\gamma^*$, where f is the frequency of the first harmonic, $\gamma^* = \delta f/\delta H_0$ is the differential value of the gyromagnetic ratio γ for the electron spin obtained allowing for the internal fields, and H_0 is the external field. The MAR was manifested as a sharp increase in the absorption of the second acoustic harmonic initially in the resonance field of the first harmonic H_{1r} and then in the field of the second harmonic $H_{2r} = H_{1r} + \Delta H_d$. A giant increase in the effective acoustic nonlinearity in the MAR region was first established in Ref. 9. The study reported in Ref. 9 and several of the subsequent investigations[10–15] were carried out at lower frequencies of $\sim 10^7$ Hz using ferrite crystals (YIG and an Mn–Zn spinel—MZS) for which the width ΔH_i of the intrinsic ferromagnetic resonance was small,[1)] when it was possible to observe both the linear and nonlinear MAR (using the second and higher harmonics).

1. CONDITIONS FOR THE EXCITATION OF A MAGNETOACOUSTIC RESONANCE AND LINE PROFILES OF MAGNETIC MATERIALS WITH INHOMOGENEOUS INTERNAL FIELDS

It is known that in the case of electromagnetic excitation of spin waves in inhomogeneous internal fields the resonance regions in which electromagnetic and spin waves are strongly coupled (turning points) are localized in space and are shifted relative to the points of phase matching between spin and elastic waves.[8] Under MAR conditions these points coincide. It is of interest to identify the local conditions necessary for the attainment of an acoustic resonance in terms of external and internal fields. It follows from the Landau-Lifshitz equation that the spin precesses around the direction of the effective field $\mathbf{H}_{eff}$ which is in general a vector sum of the exchange, the external, and all the relativistic internal fields. We shall separate the external field in the expression for the effective field:

$$\mathbf{H}_{eff} = \mathbf{n}f/\gamma = \mathbf{H}_0 + \mathbf{H}_{int} .$$

Here, $\mathbf{n}$ is a unit vector; f is the resonance frequency, $\mathbf{H}_{int}$ is the internal field. A resonance occurs when the oscillating magnetic field h created by an acoustic wave through magnetostriction is not parallel to the effective field: $\mathbf{h} \times \mathbf{H}_{eff} \neq 0$; we shall assume that this condition is satisfied.

If f/γ is given and it determines the radius of the sphere of possible values of $\mathbf{H}_{eff}$ (Fig. 1), it is obvious that the angle β between $\mathbf{H}_0$ and $\mathbf{H}_{int}$ can be found from

$$\sin \beta = \frac{1}{2H_0 H_{int}} \left[2\frac{f^2}{\gamma^2}(H_0^2 + H_{int}^2) - \frac{f^4}{\gamma^4} - (H_0^2 - H_{int}^2)^2 \right]^{1/2} .$$

(1)

In a strongly magnetized crystal ($H_0 \gg H_{int}$) when $f = \pm \gamma H_0$ (microwave MAR), the collinearity of the external and internal fields follows in a natural manner from Eq. (1): $\beta = 0$. However, under real conditions even at frequencies $f \sim 10^8$–10^9 Hz a resonance is observed in average fields $H_0 \gtrsim H_{int}$ (hf resonance) and the maximum permissible angle between the fields β_{max} is found from the condition
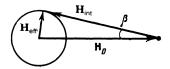
FIG. 1. Formation of the effective field H_{eff}.
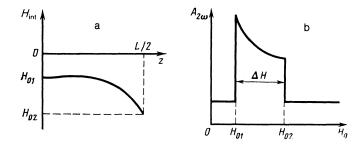

FIG. 2. Distribution of the internal field $H_{int}(z)$ along a crystal (a) and the corresponding resonance profile (b).

$$\sin \beta_{max} = f/\gamma H_0, \qquad (2)$$

i.e., β_{max} increases with frequency. In the case of lf MAR we have $|H_0| \sim H_{int} | \gg f/\gamma$, the angle β_{max} is small, and we find from Eq. (1) that $f/\gamma = \pm (H_0 \pm H_{int})$. Out of the four roots of the radicand in Eq. (1), only $f/\gamma = \pm (H_0 - H_{int})$ have physical meaning and, consequently, apart from the small resonance field, we have

$$H_0 \approx -H_{int}. \qquad (3)$$

In other words, the conditions for lf resonance are satisfied in the case of local saturation magnetization. In contrast to the widely used magnetic methods for the determination of the average magnetization of a sample, the MAR makes it possible to determine the local saturation field.

When the external field is varied in a magnetic material with an inhomogeneous H_{int}, a resonance occurs consecutively in different regions of a crystal and the structure of the internal field is scanned by the natural ferromagnetic resonance line (of width ΔH_i). In this case we can determine the size δz of the resonance region and the MAR profile or, conversely, we can use the experimental form of the profile to find $H_{int}(z)$. Because of the approximate equality given by Eq. (3), we shall ignore the difference between H_0 and H_{int}. The size δz corresponding to a small width ΔH_i can clearly be found from the expansion

$$\Delta H_i = H(z) - H(z + \delta z) = -H'\delta z - \tfrac{1}{2}H''\delta z^2 - \dots . \qquad (4)$$

Outside extrema and inflection points of the field, we have

$$\delta z = -\Delta H_i / H'. \qquad (5)$$

At field extrema, we find that

$$\delta z = (-2\Delta H_i / H'')^{1/2} \approx r_0 (\Delta H_i / H^*)^{1/2}, \qquad (6)$$

where H^* and r_0 are the characteristic local field and the radius of its action. The relationships (5) and (6) determine the local nature of the resonance. The derivatives H' and H'' can be determined approximately from the experimental MAR profile (this is discussed later), but an estimate of δz can be obtained more conveniently in a different way. In the case of a model parabolic field

$$H_{int}(z) = -H_{int}(0) - az^2$$

($z = 0$ is the center of the crystal, $0 \leqslant z \leqslant L/2$, and L is the length of the crystal), the size of the resonance region outside the extrema and inflection points is given by the relation

$$\delta z = (L^2/8z)(\Delta H_i / \Delta H), \qquad (7)$$

whereas at the extrema we have

$$\delta z = \tfrac{1}{2} L (\Delta H_i / \Delta H)^{1/2}, \qquad (8)$$

where $\Delta H = |H_{int}(L/2) - H_{int}(0)|$ is the width of the MAR profile (Fig. 2b).

A linear magnetoacoustic spectrum $A_\omega(H_0)$, where A_ω is the amplitude of an acoustic pulse transmitted by a crystal, is clearly governed by the relationship

$$A_\omega(H_0) = A_\omega(0) \exp(-2\Delta \alpha \delta z), \qquad (9)$$

where $A_\omega(0)$ is the amplitude of a transmitted pulse outside the resonance; $\Delta \alpha = \alpha_r - \alpha$; α_r and α are, respectively, the absorption coefficient of sound at the resonance and away from it. In the case of a nonlinear spectrum (at the second harmonic) we shall temporarily ignore its doublet nature and assume that the nonlinear parameter[2] at the resonance satisfies $\Gamma_r \gg \Gamma$ and $\alpha_r \gg \alpha$, which yields the following expression obtained in the approximation of the quadratic frequency dependence of the damping:

$$A_{2\omega} \sim (\Gamma_r/\alpha_r)[\exp(-2\alpha_r\delta z) - \exp(-4\alpha_r\delta z). \qquad (10)$$

If

$$2\alpha_r\delta z \ll 1, \qquad (11)$$

which—according to Eq. (5)—is valid at least in regions with high internal field gradients, we find that

$$A_\omega(H_0) \sim -2\alpha_r\delta z, \quad A_{2\omega}(H_0) \sim 2\Gamma_r\delta z.$$

The absorption at a resonance is known to be due to the increase in the magnetoelastic coupling and effective energy dissipation in a magnetic subsystem. On the other hand, the mechanism which causes Γ_r to increase is also due to resonant enhancement of the magnetoelastic coupling, the nonlinearity of this coupling, and particularly the nonlinearity of the magnetic subsystem. It is qualitatively clear that all these factors for the increase in Γ_r should also increase the damping α_r.

The condition of Eq. (11) may not be satisfied in the case of wide extrema of $H_{int}(z)$, particularly in the case of crystals with fairly strong magnetoelastic coupling, with a long spin precession relaxation time τ, and, consequently, with a strong resonant increase in the absorption. The profile $A_\omega(H_0)$ then represents the spectrum $\alpha(H_0)$ in a distorted manner, and the profile $A_{2\omega}(H_0)$ represents the spectrum $\Gamma(H_0)$. It is clear from Eq. (10) that these dissipative distortions of the spectrum begin to manifest themselves particularly strongly beyond a distance equal to the stabilization length of the second harmonic, i.e., when

$$2\alpha_r\delta z \gtrsim 0.5 \ln 2 = 0.35. \qquad (12)$$

L. K. Zarembo and S. N. Karpachev   856

The nonlinear absorption due to strong generation of higher harmonics of a magnetoelastic wave then begins to play the dominant role in the resonance region.

The relations (5), (6) and (9), (10) link the line profile with the field distribution. When $H_{int}(z)$ is given we can readily find the MAR profile from these relationships and conversely we can use $A_\omega(H_0)$ or $A_{2\omega}(H_0)$ to reconstruct $H_{int}(z)$. A unique reconstruction is possible only if the function $H_{int}(z)$ is single-valued in the interval $0 \leqslant z \leqslant L/2$ provided also that $H_{int}(z) = H_{int}(-z)$. For example, Fig. 2a shows the characteristic form of $H_{int}(z)$ and the corresponding profile of $A_{2\omega}(H_0)$ (Fig. 2b). The MAR occurs in a field H_{01} equal to the internal field $H_{int}(z)$ at the center of the crystal and then $A_{2\omega}$ decreases in accordance with the variation of $H_{int}(z)$ and, finally, the MAR disappears at the boundary of the crystal in a field $H_{02} = H_{int}(L/2)$; the width of the profile is ΔH. We shall call this the canonical profile, which is obtained in a given internal field $H_{int}(z)$ that does not vary in the course of magnetization. As pointed out above, the resonance occurs under conditions of local magnetization almost to saturation; when the resonance conditions are attained in a cross section z_0 ($0 < z_0 < L/2$), the region $z < z_0$ is practically magnetized, in contrast to $z > z_0$. In spite of this assumption, and the assumed one-dimensional nature of $H_{int}(z)$, measurements on long and particularly thin ferrite samples yield near-canonical profiles of the linear and nonlinear S-MAR (S denotes transverse waves) in contrast to the L-MAR (longitudinal waves): the profile is characterized by an abrupt leading edge and it exhibits a characteristic asymmetry (see below).

It follows from the above discussion and also from actual experiments that lf MAR occurs in fields somewhat less than the saturation magnetization fields, so that resonance excitation is superposed on the modification of the domain structure: domain walls are displaced and the magnetization vector is rotated. The polydomain nature of a crystal strongly affects the damping, i.e., it influences the magnetic spectrum $A_\omega(H_0)$; in some cases it is found experimentally that the lf resonance can no longer be observed. Under these conditions the strong domain damping of sound sometimes makes it difficult even to observe the nonlinear MAR on the basis of the second or higher harmonics. In the saturation region the domain damping disappears and the crystal becomes "transparent," but the local electric fields exceed the resonance value at the selected frequency throughout the crystal.

The possibility of observing magnetically charged defects by a resonance method is of practical interest. Fairly strong inhomogeneous exchange fields are likely to exist near defects. Therefore, the resonance conditions in the region of a defect should be attained in external fields exceeding the saturation field. However, in view of the small radius of action r_0 and of the high value of H^* in Eq. (6), these regions have small sizes δz and should be largely smeared out in the magnetic spectrum $A_\omega(H_0)$. This masking of small high-field defects prevents us from finding their positions: the influence of such defects can be manifested only in the background magnetic absorption in the saturation region.

Naturally, the observation of the MAR is possible only if

$$f\tau > 1. \tag{13}$$

This condition limits both the MAR frequency (from below) and the class of objects in which the resonance can be observed to crystals with the intrinsic ferromagnetic resonance line width obeying

$$\Delta H_i < H_{eff} = f/\gamma. \tag{14}$$

In this connection it is worth mentioning certain difficulties encountered in the observation of the MAR: in the hf range we need crystals which conduct sound readily (all the investigations[1-7] in the range $f > 10^8$ Hz were carried out on YIG); on the other hand, observation of lf MAR requires not only good acoustic conductivity at these low frequencies (which extends the class of crystals that can be used compared with hf MAR), but also a narrow ferromagnetic resonance line.

Our investigation was carried out on high-quality YIG crystals and various MZS crystals. At the frequency of 30 MHz the effective field was $H_{eff} \approx 11$ Oe and the condition (13) was satisfied by YIG. In the case of MZS crystals grown by the Verneuil method[12] the ferromagnetic resonance line width was $\Delta H_i < 2$ Oe and Eq. (13) was obeyed. We also investigated MZS crystals grown by the Bridgman method for which the value of ΔH_i could not be estimated, but in the case of the majority of them (especially after annealing which reduced the domain damping) it was possible to observe the MAR clearly, which indicated [on the basis of Eq. (14)] that the ferromagnetic resonance line width was less than 11 Oe.

We shall end this section with an estimate of the resolvability of the nonlinear MAR doublet. This estimate can be obtained on the basis of the following considerations: if the resonance frequency is $f \approx \gamma(H_0^2 - H_{int}^2)^{1/2}$ (Ref. 16), it follows that since $\gamma^* = \partial f/\partial H_0$, then $\Delta H_d = f^2/\gamma^2 H_0$. The doublet is resolved subject to the obvious condition $\Delta H_d > \Delta H_i$, which gives

$$f\tau > H_0/H_{eff}. \tag{15}$$

This condition is more stringent than the conditions for the observation of the MAR given by Eqs. (13) and (14). At lower frequencies it ceases to be satisfied earlier than the conditions for the observation of the MAR given by Eqs. (13) and (14), and the doublet is not resolved at low frequencies. Under the experimental conditions of Ref. 7 the condition (15) was known to be satisfied, so that the doublet could be resolved quite readily. In the case of our experiments on YIG crystals and the better MZS crystals we found that $\Delta H_d \approx \Delta H_i$, so that the doublets could not be resolved even in the case of a favorable distribution of the internal field, for example in the region where a resonance line appeared.

2. EXPERIMENTS

The bulk of our experimental results were obtained at a frequency of 30 MHz, although the MAR was observed also at lower frequencies (down to 5 MHz). Ultrasonic pulses of $\approx 1.5 \mu sec$ duration were excited in crystals using quartz or $LiNbO_3$ transducers. The pulses transmitted by the crystals were also detected with piezoelectric transducers (in the case of the nonlinear MAR with the resonance frequency close to the frequency of the second harmonic). The receiver section of the apparatus had two channels for the first and

second harmonic. A pulse was selected from a series of those transmitted by a crystal and, after measurements of its parameters, the signal was applied to the Y input of an X-Y plotter. The X input of the plotter received a linearly varying current from an electromagnet (constructed as described in Ref. 17) the gap of which contained a crystal.

A cylindrical YIG crystal 7 mm in diameter and 15 mm long had its axis oriented in the [100] direction. Spinel crystals had dimensions of $3 \times 4 \times 20$ mm and different orientations of the long axis ([100], [110], [111]), which was the direction of propagation of sound. Both YIG and MZS crystals have cubic symmetry and at room temperature (measurements were made at this temperature) the first magnetic anisotropy constant of MZS was positive[18] (in this case the easy magnetization axis was [100]), whereas the corresponding constant of YIG was negative (easy magnetization axis [111].

The resonance was investigated using transverse waves (S-MAR). For these waves the [100] and [111] axes were acoustic; along [110] there was splitting into a fast transverse (FS) component with a displacement vector $\xi \parallel$ [001] and a slow transverse component (SS) with $\xi \parallel$ [110]. In cubic crystals with all these orientations the transverse wave was magnetically active (see, for example, Ref. 19): it was accompanied by a coupled wave of the magnetic field h with a component orthogonal to the wave vector k. Therefore, in a longitudinal magnetic field the magnetization of a crystal created conditions favorable for S-MAR. This resonance was observed not only in the case when $k \parallel H_0$, but also when the crystal axis was oriented at an angle θ between k and H_0. Under the S-MAR conditions the field $H_{01} = H_{int} (0)$ increased with θ (Fig. 3), which was due to an increase in the effective demagnetization coefficient. On approach to $\theta = 90°$ the resonance amplitude decreased strongly and the resonance disappeared in a transverse field $k \perp H_0$. A similar dependence was observed also for the S-MAR in a crystal of YIG.

The S-MAR was observed most clearly in MZS ($Mn_{0.68} Zn_{0.34} Fe_{1.98} O_4$) single crystals grown by the Verneuil method. These crystals were characterized by a relatively weak damping in the absence of an external field ($\alpha = 0.6$ cm^{-1}). In a magnetic field the damping (absorption) changed very little, so that the linear MAR was observed in the $A_\omega (H_0)$ spectrum only for the third transmitted pulse (Fig. 4). The MAR profile was nearly canonical. An estimate of the size of the resonance region at the center
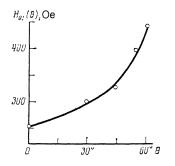
of a crystal obtained from Eq. (8) gave $\delta z = 10^{-1}$ cm, whereas Eq. (9) yielded $\Delta \alpha = 0.8$ cm^{-1}, i.e., $\alpha_r = 1.4$ cm^{-1}, and the resonance absorption was approximately twice as high as the nonresonance effect. At the center of the crystal we found that $2\alpha_r \delta z = 0.28$. Since the condition (12) was not satisfied even at the center of the crystal, the dissipative distortions of the spectrum were weak and, as demonstrated in Fig. 4, we found that $A_\omega (H_0) = -A_{2\omega} (H_0)$, in agreement with the ideas put forward earlier.

Nonlinear S-MAR ($A_{2\omega}$) was observed clearly in the Verneuil-grown MZS crystals using the first transmitted pulse (Fig. 4). Its fine structure differed from $A_\omega (H_0)$ and this could be due both to the influence of the domain structure and to the fact that the approximate relationships given above ignored the fairly strong dispersion of the velocity of sound in the region of the resonance. One should stress here once again that the spectra of A_ω and $A_{2\omega}$ represented somewhat different physical phenomena.

An increase in $A_{2\omega}$ at the resonance and in the size δz of the resonance region in the case of a Verneuil-grown MZS

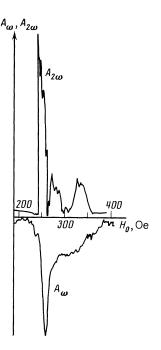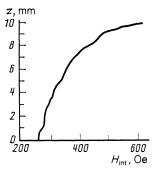
FIG. 4. Resonance parts of the magnetoacoustic $A_\omega (H_0)$ and $A_{2\omega} (H_0)$ spectra of a Verneuil-grown MZS crystal ($H_0 \parallel k \parallel$ [110]).

FIG. 3. Dependence of the field on the onset of the S-MAR on the angle θ between k and H_0 in a Verneuil-grown MZS crystal ($k \parallel$ [110]).

FIG. 5. Reconstructed distribution of the internal field along the [110] axis in a Verneuil-grown MZS crystal.
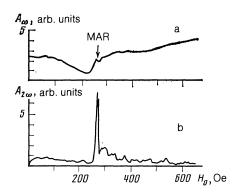
L. K. Zarembo and S. N. Karpachev   858

FIG. 6. Linear (a) and nonlinear (b) S spectra of a Bridgman-grown MZS crystal ($H_0\|k\|[100]$).

crystal could be used to estimate the resonance enhancement of the nonlinear parameter $\Gamma_r/\Gamma = 400 \pm 100$. Small dissipative distortions of the S spectra of this crystal made it possible to reconstruct the distribution of the internal field (Fig. 5) from Eqs. (5), (6,), (9), and (10).

One should point out that the domain structure in a Verneuil-grown MZS crystal was manifested only by a slight flattening of the onset of the linear MAR (Fig. 4). The influence of a highly developed domain structure on the magnetic S spectra of A_ω and $A_{2\omega}$ is demonstrated in Fig. 6, which gives these spectra for the Bridgman-grown MZS crystals which differ also in the iron concentration $Fe_{2.04-2.06}$. In the linear spectrum $A_\omega(H_0)$ the S-MAR preceded a dip which was considerable, smooth, and wide (on the field scale reduction in the amplitude) due to an increase in the domain damping during modification of the domain structure. An annealing of this crystal affected only the domain wall mobility and, therefore, the amplitude and shape of the dip: the amplitude and shape of the MAR profile were not affected.[13] The nonlinear S-MAR (Fig. 6b) had a near-canonical profile: an oscillatory structure of the signal in the range of fields exceeding $H_{02} = H_{int}(L/2)$ was due to "difficult" boundary domains. A comparison of Figs. 6a and 6b revealed an interesting feature: the dynamics of the domain structure was not reflected in the spectrum $A_{2\omega}(H_0)$ and, consequently, the quadratic domain nonlinearity was considerably less than the quadratic magnetoelastic and magnetic nonlinearities at the resonance. The cubic domain nonlinearity observed in Ref. 15 in fields less than the resonance value was probably due to the anisotropy fields.

It should be pointed out that the magnetic characteristics of YIG did not differ greatly from those of MZS, with the exception of the saturation magnetization. As pointed out already, the shapes of the samples were different. In the case of YIG the attenuation of the transverse wave traveling along the [100] axis was $\alpha = 0.4$ cm^{-1} in zero field.[9] An estimate of the line width ΔH could best be made using the profile of the nonlinear S-MAR. According to Ref. 9, the line width was $\Delta H \approx 170$–200 Oe; for $\Delta H_i = 1$ Oe at the center of the crystal, Eq. (8) gave $\delta z \approx 5 \times 10^{-2}$ cm. The average damping along a crystal was given in Ref. 9. In reality the amplitude of a transmitted pulse was given by

$$A_\omega = A_0 \exp[-\alpha(L-2\delta z)-2\alpha_r\delta z] = A_0 \exp(-\alpha^* L),$$

where α^* is the attenuation coefficient averaged over the

length of a crystal. Hence we found the resonance value $\alpha_r = (a^* - \alpha)L/2\delta z + \alpha$, which according to Ref. 9 corresponded to $\alpha_r = 21.4$ cm^{-1}, i.e., the attenuation in YIG increased by almost two orders of magnitude in the region of the S resonance (it should be stressed once again that such attenuation was local). It was then found that $2\delta z\alpha_r = 2.14$ and the inequality (12) was satisfied: the dissipative distortion of the profiles of the linear and nonlinear MAR was fairly strong. This is illustrated also in Fig. 7: the magnetic spectrum of the second harmonic $A_{2\omega}$ had a maximum not at the center of the crystal but closer to its edges (it was estimated that this maximum was located at ≈ 2 mm from the ends of the crystal), where the dimensions of the resonance region δz were comparable with the stabilization distance $\ln 2/2\alpha_r$ for the second harmonic. The profile of the linear S-MAR (curve a) was close to canonical, but it was distorted by the influence of the domain and resonance damping. Our earlier determination[9] of the resonant increase in the nonlinear parameter of YIG was made on the assumption that the nonlinear distortions occurred throughout the crystal. In view of the local nature of the resonance regions, a giant increase in Γ_r was observed, estimated to be between five and six orders of magnitude. The dissipative distortions in the regions near the center of the crystal were large and, therefore, the received harmonic was small, but near the ends of the crystal there were regions where the competition between the resonance damping and the nonlinearity was won by the latter, resulting in a strong increase in the amplitude of the received second harmonic.

We can summarize the results by saying that the large differences between the nature of the linear S-MAR spectra obtained for YIG and MZS samples were mainly due to the difference between the magnetoelastic nonlinearity (since the magnetoelastic constants normalized to the saturation magnetization M_0 were approximately of the same order of magnitude) and the nonlinearity of the magnetic subsystem. In practice the only physical parameter different for these two crystals was M_0 (it was three times greater for MZS than for YIG). Physically it was obvious that the magnetic moments with large absolute values would be difficult to set in motion and, consequently, the nonlinear distortions should be less because of the smaller amplitude. This was clear from, for example, the Bloch–Landau equation (see, for example, Ref. 8) in which the term due to the exchange interaction occurred in the denominator M_0. Under otherwise constant conditions (the exchange constants of these mate-
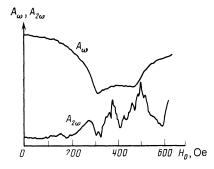

FIG. 7. Linear (A_ω) and nonlinear $(A_{2\omega})$ S spectra of YIG ($H_0\|k\|[100]$).

L. K. Zarembo and S. N. Karpachev   859

rials were also similar, as deduced from the similarity of the Curie temperatures of the two materials: $T_c = 470$ K for MZS and 550 K for YIG) this reduced the resonance magnetic nonlinearity, as confirmed also by the estimates given above.

---

[1] Here and below ΔH_i is understood to be the line width due to the spin–spin and spin–lattice interactions in the presence of a homogeneous internal field.

[2] In the physical nonlinearity approximation the nonlinear parameter is the ratio, for a given type of wave, of the combination of the effective third-order elastic moduli to the effective second-order moduli.

---

[1] A. I. Akhiezer, V. G. Bar'yakhtar, and S. V. Peletminskii, *Spin Waves*, North-Holland, Amsterdam; Wiley, New York (1968).

[2] B. Lüthi, Phys. Lett. 3, 285 (1963).

[3] G. A. Smolenskiĭ and A. Nasyrov, Fiz. Tverd. Tela (Leningrad) 7, 3704 (1965) [Sov. Phys. Solid State 7, 3002 (1966)].

[4] M. F. Lewis and D. G. Scotter, Phys. Lett. A 28, 303 (1968).

[5] V. V. Lemanov and A. V. Pavlenko, Zh. Eksp. Teor. Fiz. 57, 1528 (1969) [Sov. Phys. JETP 30, 826 (1970)].

[6] V. V. Lemanov, A. V. Pavlenko, and A. N. Grishmanovskiĭ, Zh. Eksp. Teor. Fiz. 59, 712 (1970) [Sov. Phys. JETP 32, 389 (1971)].

[7] A. N. Grishmanovskiĭ, N. K. Yushin, V. L. Bogdanov, and V. V. Lemanov, Fiz. Tverd. Tela (Leningrad) 13, 1833 (1971) [Sov. Phys. Solid State 13, 1537 (1971)].

[8] W. Strauss, in: *Physical Acoustics: Principles and Methods* (ed. by W. P. Mason), Vol. 4B, Academic Press, New York (1968), p. 211.

[9] L. K. Zarembo, S. N. Karpachev, and S. Sh. Gendelev, Pis'ma Zh. Tekh. Fiz. 9, 502 (1983) [Sov. Tech. Phys. Lett. 9, 217 (1983)].

[10] L. K. Zarembo and S. N. Karpachev, Fiz. Tverd. Tela (Leningrad) 25, 2343 (1983) [Sov. Phys. Solid State 25, 1345 (1983)].

[11] L. K. Zarembo and S. N. Karpachev, Fiz. Tverd. Tela (Leningrad) 26, 1943 (1984) [Sov. Phys. Solid State 26, 1178 (1984)].

[12] L. K. Zarembo, S. N. Karpachev, and S. Sh. Gendelev, Pis'ma Zh. Tekh. Fiz. 10, 1050 (1984) [Sov. Tech. Phys. Lett. 10, 442 (1984)].

[13] S. G. Abarenkova, S. Sh. Gendelev, L. K. Zarembo, S. N. Karpachev, A. A. Pankov, and M. A. Kharinskaya, Fiz. Tverd. Tela (Leningrad) 27, 2450 (1985) [Sov. Phys. Solid State 27, 1467 (1985)].

[14] L. K. Zarembo and S. N. Karpachev, Fiz. Tverd. Tela (Leningrad) 28, 311 (1986) [Sov. Phys. Solid State 28, 173 (1986)].

[15] O. Yu. Belyaeva, L. K. Zarembo, and S. N. Karpachev, Vestn. Mosk. Univ. Fiz. Astron. 28, 50 (1987).

[16] B. Lax and K. J. Button, *Microwave Ferrites and Ferrimagnetics*, McGraw-Hill, New York (1962).

[17] S. P. Kapitsa, Prib. Tekh. Eksp. No. 2, 97 (1958).

[18] Y. Kawai and T. Ogawa, Phys. Status Solidi A 76, 375 (1983).

[19] B. A. Auld, Appl. Solid State Sci. 2, 1 (1971).

Translated by A. Tybulewicz

860   Sov. Phys. JETP 66 (4), October 1987

L. K. Zarembo and S. N. Karpachev   860